PHYSICAL REVIEW E **74**, 051706 (2006)

Experimental demonstration, using polarized Raman and infrared spectroscopy, that both conventional and de Vries smectic-*A* phases may exist in smectic liquid crystals with a first-order *A*-C^* transition

Naoki Hayashi,[1] A. Kocot,[2,3] M. J. Linehan,[2] Atsuo Fukuda,[2,4] Jagdish K. Vij,[2,*] G. Heppke,[5] J. Naciri,[6] Sachiko Kawada,[7] and Shinya Kondoh[7]
[1] *Institute for Molecular Science, Myodaiji, Okazaki 444-8585, Japan*
[2] *Department of Electronic and Electrical Engineering, Trinity College, University of Dublin, Dublin 2, Ireland*
[3] *Institute of Physics, Silesian University, Silesia, Katowice, Poland*
[4] *Department of Environmental Materials Science, Tokyo Denki University, Tokyo 101-8457, Japan*
[5] *Iwan-N-Stranski-Institut, Technische Universität Berlin, Sekretariat ER 11, Strasse des 17, Juni 135, D-10623 Berlin, Germany*
[6] *Naval Research Laboratory, Code 6900, 4555 Overlook Avenue South West, Washington, D.C. 20375, USA*
[7] *Citizen Watch Co., Ltd., Tokorozawa 359-8511, Japan*

(Received 21 October 2005; revised manuscript received 7 April 2006; published 16 November 2006)

Two models exist for the orientational distribution of the long molecular axes in smectic-*A* liquid crystals: the conventional unimodal distribution and the "cone-shaped" de Vries distribution. The de Vries hypothesis provides a plausible picture of how, at a molecular level, a first-order Sm-*A* to Sm-C^* transition may occur, especially if there is little or no concomitant shrinkage of the layer spacing. This work investigates two materials with such transitions: C7 and TSiKN65. The azimuthal distribution of in-layer directors is probed using IR and polarized Raman spectroscopy, which allows us to obtain orientational order parameters. In C7, we observe a discontinuous change in the order parameter, the magnitude of which is small compared with the corresponding change in the in-layer director tilt angle Θ. Assuming that the smectic-*A* liquid crystal is of the de Vries type, we calculate the Θ required to reproduce the apparent order parameter $\langle P_2\rangle_{\mathrm{app}}$, obtained from IR, by using the true order parameter $\langle P_2\rangle$, obtained from polarized Raman scattering. The results indicate that, for C7, the tilt angle so calculated is much smaller than that in the Sm-C^* angle and hence de Vries behavior may not be the appropriate explanation in this case. Conversely, we find that TSiKN65 shows a different behavior to C7, which can be explained in terms of the de Vries concept. Thus, we conclude that either type of distribution may exist in Sm-*A* phases which undergo a first-order transition to the Sm-C^* phase. We also discuss the changes in the smectic layer spacing and the orientational order parameters across the Sm-*A*-Sm-C^* phase transition, together with changes in birefringence with applied electric field.

DOI: 10.1103/PhysRevE.74.051706 PACS number(s): 61.30.Eb, 64.70.Md, 77.80.Bh, 77.84.Nh

I. INTRODUCTION

A rod-shaped molecular system may form smectic-*A* and/or smectic-*C* liquid crystals (Sm-*A* and/or Sm-*C*), which are orientationally ordered fluids with a one-dimensional density wave. The phase structure can also be regarded as an arrangement of rod-shaped molecules in smectic layers, though not definitely defined as in layered solid crystals. The wave vector is parallel to the smectic layer normal $\hat{\boldsymbol{e}}$, and the definiteness of the smectic layer is specified by positional order parameters. As in nematic liquid crystals, the *director* $\hat{\boldsymbol{n}}$ is usually defined as the averaged direction of the long axes of the constituent molecules and the orientational order parameters are introduced to specify the orientational distribution of the long axes around the director. The director in Sm-*A* is parallel to the smectic layer normal, while it is tilted and makes an angle of Θ in Sm-*C*. When the molecules are optically active, the chiral smectic-*C* phase (Sm-C^*) is observed; ferroelectricity emerges with spontaneous polarization perpendicular to the tilt plane defined by $\hat{\boldsymbol{e}}$ and $\hat{\boldsymbol{n}}$, and the director forms helicoidal structure with a pitch on the μm scale and the axis parallel to $\hat{\boldsymbol{e}}$. The Sm-*A*-Sm-C^* phase transition is mainly driven by intermolecular interactions producing Sm-C^* and not by a ferroelectric coupling between the permanent dipoles. Thus the spontaneous polarization in Sm-C^* is not the primary order parameter.

Various molecular models for Sm-*C* have been proposed since the 1970s, and these have tried to reveal different factors which may be responsible for the tilt. Among them, a model proposed by van der Meer and Vertogen [1] seems to be realistic, which is based on the electrostatic interaction between the off-center dipole and the polarizability of neighboring molecules. Recently Govind and Madhusudana [2,3] modified this model. They based their model on the physical basis of the molecular structures of the compounds that lead to the formation of Sm-C^* phase. They consider interactions between the dipoles that are situated off the central axis of the neighboring molecules and assume that the polarizability of the molecules lies at their centers. In spite of the difference in the manner in which the particular interactions are taken into account by different models, the corresponding model interaction potentials are similar from the mathematical point of view and they all have the symmetry of the quadrupole-quadrupole interaction [2–8]. Accumulated experimental and theoretical investigations led to a conclusion that the Sm-*A*-Sm-*C* phase transition may not be of the

---

[*] Author to whom correspondence should be addressed. Electronic address: jvij@tcd.ie

disorder-order type with the director tilt $\Theta \exp(i\Phi)$ as the primary order parameter [9]. It should be noted, however, that the disorder-order aspect was emphasized in the early stages of investigation in connection with either the molecular biaxiality [10–13] or a small change in the smectic layer spacing occurring at the Sm-A to Sm-C^* transition [14–20]. The biaxiality is still believed to be a result, but not a cause, of the director tilting in Sm-C. In fact, Priest showed that even an idealized system of uniaxial molecules may form Sm-C [4]. On the contrary, the small change in the layer spacing has received renewed interest due to the recognition of the extremely reduced tilting correlation between the adjacent layers in antiferroelectric liquid crystals (Sm-C_A^*). Its importance has also been emphasized in the manufacture of the high-quality electro-optic devices based on ferroelectric or antiferroelectric liquid crystals.

Two papers published in 1977 by de Jeu and de Poorter [15] and by de Vries [16] reported that the Sm-A-Sm-C phase transition in two compounds they investigated would be of disorder-order type since the smectic layer spacing determined by x-ray diffraction scarcely showed a temperature variation. They concluded that the molecular long axis is tilted from the smectic layer normal $\hat{\boldsymbol{e}}$ by 15°–17° in both Sm-A and Sm-C. In fact, most molecules make quite large angles with the smectic layer normal in Sm-A because the orientational order parameter $S=\langle P_2\rangle$ is significantly less than unity; for $S=0.8$, the average molecular tilt angle is about 19°. In his later publications [18–20], de Vries introduced "the diffuse-cone model" and "the preferred angle θ_m between the molecular long axes and the smectic layer normal." Although the term "director" could not be found in his papers, the distribution function de Vries used (Eq. 2 in Ref. [19]) indicates that he actually considered the director. Consequently, we can summarize the disorder-order aspect of the Sm-A-Sm-C phase transition he intended to emphasize as follows: The director is tilted from $\hat{\boldsymbol{e}}$ by an angle of Θ even in Sm-A, but it distributes randomly around $\hat{\boldsymbol{e}}$ to assure the uniaxiality of Sm-A. Such a Sm-A is completely different from ordinary Sm-A. This is a tilted phase and hence belongs to the Sm-C family, although it has been designated as de Vries Sm-A for convenience. Since the director tilts in a single direction in Sm-C, the apparent orientational ordering of molecular long axes is expected to become higher in Sm-C than in de Vries Sm-A.

Suppose $\Theta=\text{const}$ during the phase transition; it is understandable that the smectic layer spacing does not change. But how can we envisage the existence of de Vries Sm-A? In his first paper about this topic, de Vries suggested an "uncoupling of the tilt directions of adjacent layers" [16]. The density-wave character of smectic layers, as had been established at the time, made it difficult to accept the concept of uncoupling. The discovery of anticlinic antiferroelectric Sm-C_A^*, however, did remove this difficulty, at least in principle [21]. The tilting correlation of the in-layer directors in adjacent layers is reduced in Sm-C_A^*, because the smectic layer is well defined [22,23] and the free energy difference between synclinic ferroelectric Sm-C^* and anticlinic antiferroelectirc Sm-C_A^* is very small [8,24,25]. The phase transition from Sm-C_A^* to Sm-C^* can easily be induced by a moderate electric field $E \sim 10^5$ V m^{-1}. This means that the Sm-C_A^* can also be strongly affected by other macroscopic factors including substrate boundary conditions [26–28]. In fact, Langevin-like director reorientation was observed in an interface-induced disordered Sm-C^*-like state (designated as Sm-C_R^*, where the suffix R refers to "random distribution of $\hat{\boldsymbol{n}}$ around $\hat{\boldsymbol{e}}$") [29–32]. It should be noted that Sm-C_R^* was originally proposed by Fukuda and by Inui *et al.* in connection with the "V-shaped switching" [33,34]. More recently, the Sm-A phase in the bulk of some liquid crystals has been reported to be of the de Vries type [35–37]. The sliding phase reported recently is an analog of Sm-C_R^* or de Vries Sm-A in lyotropic liquid crystals [38]. A significantly different phase was proposed by de Vries *et al.* [18,37,39,40,42] which is now believed to be what de Vries thought was the correct phase, which he intended to introduce to explain his experimental observations [43]. In this phase, the in-layer directors are tilted but the tilting direction specified by the azimuthal angle varies even in a single layer. Here it is natural to consider the local in-layer directors. Meyer and Percovits [44] showed that the system will form a modulated Sm-C^* phase consisting of a regular network of defect walls and possibly points. If the spacing of these defects is in the subvisible range, this modulated Sm-C^* phase should look like de Vries Sm-A. The spacing between such defects has not yet been observed in the uv-visible spectral region as the experiment on the circular dichroism did not give any signal on a compound that showed de Vries Sm-A phase.

The purpose of this paper is to determine the director's azimuthal distribution and to confirm whether or not a de Vries Sm-A phase exists in either of two materials: TSiKN65 and 4-(3-methyl-2-chloropentanoyloxy)4′-heptyloxybiphenyl (C7). The second compound C7 belongs to a family of chiral smectic materials that show a first-order Sm-A to Sm-C^* transition. We first obtain apparent orientational order parameters by using IR and polarized Raman spectroscopy in Secs. II A and II B. At the phase transition to Sm-C^*, a discontinuous increase in the order parameters is actually observed in C7 but the change is rather small as compared with a large jump in the tilt angle. Then in Sec. III we calculate the corresponding apparent orientational order parameters by assuming de Vries Sm-A with appropriate Θ. By comparing the calculated and experimentally obtained $\langle P_2\rangle_{\text{app}}$ and $\langle P_4\rangle_{\text{app}}$, we try to separate out the fluctuational molecular tilt and the real director tilt. The results indicate that for C7 there in no need to consider the existence of de Vries behavior. This type of phase is possibly present in only some siloxane-based materials or compounds with large tilt angles [36,40,42,45]. In other words, the established models for ordinary Sm-A and SmC^* may be sufficient for reproducing the observed order parameters and for describing the phase transition in some of the compounds that also show a first-order Sm-A to Sm-C^* transition. We discuss the changes in the smectic layer spacing and in the order parameters across the Sm-A-Sm-C^* phase transition and a change in the birefringence with the electric field. We compare and contrast the results obtained for C7 with a recently reputed de Vries material TSiKN65.

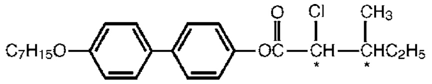

isotropic - 62 °C - Sm-*A** - 52 °C - Sm-*C** - 45 °C - Sm-*G**

FIG. 1. Chemical structure and phase sequence of the liquid crystal 4-(3-methyl-2-chloropentanoyloxy)4′-heptyloxybiphenyl abbreviated as C7.

II. EXPERIMENT AND RESULTS

A. Infrared spectroscopy in homeotropically and homogeneously aligned cells

A cell for infrared measurements was prepared using ZnSe windows and a Mylar spacer of thickness 6.3 μm. Homeotropic alignment of C7 was obtained by coating the windows of the cell with chromolane films cured at 120 °C. The cell was filled with the sample compound in its isotropic phase. The chemical structure and phase sequence are given in Fig. 1. The texture of the sample observed under a polarizing microscope confirmed an excellent homeotropic alignment in Sm-*A*; it was found to be a single-domain texture. After the phase transition into Sm-C^*, it became multidomain texture (domains with different azimuthal angles at the surface). This is due to the azimuthal freedom of tilting directions. This implies that the azimuthal angle of the director can take all possible angles with equal probability from 0 to 2π on the surface of the film. This is confirmed by the absence of IR dichroism. The absorbance when integrated over the area of the IR beam (diameter of the beam $\leqslant 10$ μm) is independent of the projection of the director on the plane of the window. The IR absorbance measurements were carried out in the transmission mode with a temperature step of 0.5 K using a Fourier transform infrared Bio-Rad FTS-6000 spectrometer equipped with a fast MCT detector. For the homeotropically aligned sample in the Sm-*A* phase, IR dichroism was also absent for the reason already given; hence there was no need for the use of a polarizer for this part of the experiment. The spectra were averaged over 32 scans. The absorbance band of the phenyl ring C-C stretching mode at 1608 cm^{-1} was then fitted using a Voigt function and the integrated area under the absorbance band was obtained.

Figure 2 shows the normalized area under the absorbance band, $A_\perp/A_{\text{iso}}$, in the homeotropically aligned sample. This ratio is proportional to the projection of the square of the transition moments in perpendicular direction to the layer normal in the liquid crystalline phases to that of the isotropic phase. In this experiment, the IR beam is incident along the layer normal. Here $A_{\text{iso}}=4.29$ cm^{-1} is the area under the absorbance band in the isotropic phase (iso) and $A_\perp$ is the corresponding area in Sm-*A*, Sm-C^*, and Sm-G^*. The area in the absorbance band has the same units as that of abscissa since the ordinate is dimensionless. The transition dipole of the phenyl ring C-C stretching mode is nearly parallel to the molecular long axis. On cooling from isotropic to Sm-*A*, a sudden drop in the normalized absorbance area $A_\perp/A_{\text{iso}}$ is observed. This implies a drop in the projections of the square of the transition moments normal to the direction of the IR beam. This observation is consistent with the excellent homeotropic alignment in Sm-*A* and shows that the long molecular axes are highly aligned along the direction perpendicular to the substrates of the sample cell. It should be noted that $A_\perp/A_{\text{iso}}$ decreases gradually as the temperature falls in Sm-*A*. Intuitively, this decrease suggests that "Sm-*A*" under consideration is of ordinary but not of de Vries type. Details will be discussed in Sec. III. At the phase transition to Sm-C^*, an abrupt increase in $A_\perp/A_{\text{iso}}$ is observed. This is a consequence of the director tilting by Θ from the smectic layer normal $\hat{\boldsymbol{e}}$. The transition dipole of the phenyl ring C-C stretching mode would directly contribute to the measured absorbance. As Θ becomes larger on cooling in Sm-C^*, this contribution increases with a further decrease in temperature. We also plot $A_\parallel$, for which the measurements are made on a homogeneously aligned cell using a polarizer in this part of the IR experiment. The transition moment under consideration is again for the phenyl stretching band. A uniform domain emerges for the SSFLC state as only one of the cell surfaces is rubbed since the cell is asymmetrical (only one of the cell surfaces is rubbed). The director of this SSFLC state lies in the plane of the substrate. The polarizer is rotated until its position coincides with the director; hence, the absorbance is measured in a direction parallel to the director. The absorbance increases from the isotropic to Sm-*A* phase as expected. There is also a jump in the absorbance at the Sm-*A* to Sm-C^* transition, which obviously is due to a jump in the order parameter. There is an increase in the absorbance with a reduction in temperature in both Sm-*A* and Sm-C^* phases due to a gradual increase in the order parameter with a reduction in temperature. The shift of the director from the layer normal by an angle Θ is not seen in Sm-C^* for the case of homogeneous configuration of the cell as the polarizer is rotated to follow the director. The absorbance and consequently the order parameter are thus independent of Θ. The experimental facts are that (i) the absorbance does not change much in Sm-*A* and Sm-C^* apart from that expected from the temperature variations in both cases of the homeotropic and homogeneous configurations and (ii) a change in the absorbance occurs only at the Sm*A* to Sm-C^* transition. These two observations indicate that Sm-*A* phase under consideration is an orthogonal and not a de Vries type and furthermore Sm-C^* is also a conventional type of phase.

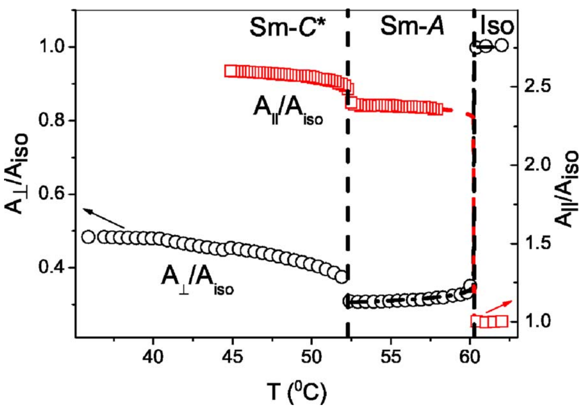

FIG. 2. (Color online) IR absorbance of phenyl stretching band (1608 cm^{-1}) in the homeotropic and homogeneous alignment of the liquid crystalline compound C7.

For comparison, an essentially identical IR experiment was conducted on a homeotropic cell filled with the liquid

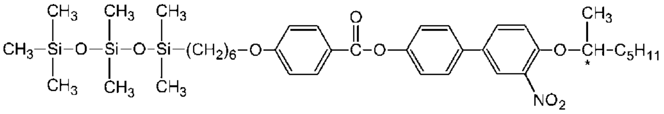

SmC* - 25 °C – SmA* – 56 °C – Isotropic

FIG. 3. Chemical structure and phase sequence of 4-[3′-nitro-4′-(R)-1(methylhexyloxy)phenyl]phenyl 4-(6-heptylmethoxyltrisiloxyhexyloxy)benzoate (TSiKN65).

crystal TSiKN65 (Fig. 3) synthesized by Naciri *et al.* [46] and studied first by Spector *et al.* [39]. This material also undergoes a first-order Sm-*A*-Sm-C^* transition. The results for $A_\perp/A_{\text{iso}}$, again for the phenyl ring C-C stretching mode at 1608 cm^{-1}, are shown in Fig. 4. The sharp drop in normalized absorbance area at the isotropic to Sm-*A* transition again demonstrates that the sample has excellent homeotropic alignment. However, in this case the absorbance increases with decreasing temperature in the Sm-*A* phase. This suggests that TSiKN65 displays de Vries–type behavior in which the molecules become progressively more tilted as the Sm-*A* phase cools towards the Sm-C^* phase. Furthermore, there is essentially no discontinuity in the absorbance (and hence the molecular tilt) at the Sm-*A* to Sm-C^* transition point, although the tilt then smoothly increases with decreasing temperature in the Sm-C^* phase, as one conventionally expects.

Let us obtain the apparent orientational order parameter $S_{\text{app}}=\langle P_2\rangle_{\text{app}}$ in Sm-*A* and Sm-C^* and the director tilt in Sm-C^* from the results of the measurements on a homeotropically aligned cell. Merkel *et al.* [47] have derived the following equation for the infrared absorbance with the IR beam incident normally to the substrates in a homeotropically aligned liquid crystal cell configuration:

$$A_\perp/A_{\text{iso}} = 1 + S_{\text{app}}\left(\frac{3}{2}\sin^2\beta - 1\right) + \frac{1}{2}D_{\text{app}}\sin^2\beta\cos 2\phi, \tag{1}$$

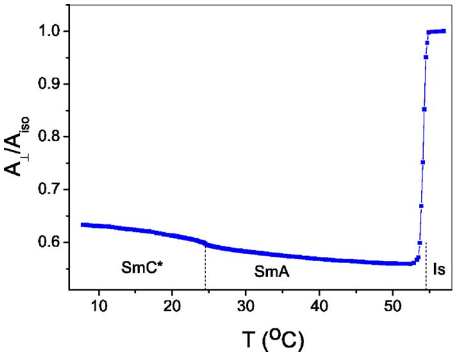

FIG. 4. (Color online) IR absorbance of phenyl stretching band (1608 cm^{-1}) in the homeotropically aligned liquid crystal TSiKN65.

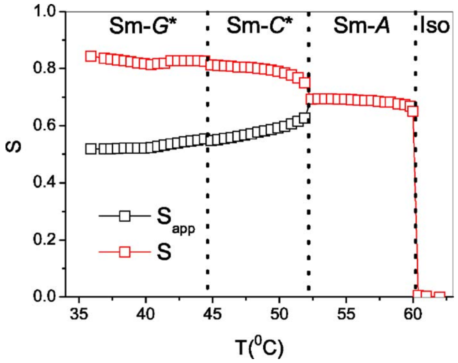

FIG. 5. (Color online) Apparent orientational order parameter S_{app} and molecular S order parameters obtained from the IR experiments for C7.

where β and ϕ are the angles that specify the direction of the IR transition dipole moment with respect to the long and short molecular axes in the molecular frame of reference, and S_{app} and D_{app} are the apparent orientational order parameters for the long and short molecular axes, respectively. For the phenyl ring C-C stretching mode, β is typically less than 6°, and hence the terms proportional to $\sin^2\beta$ can be neglected. This amounts to a negligible error of approximately 1% in the determination of S_{app}. We obtain

$$S_{\text{app}} = 1 - A_\perp/A_{\text{iso}}, \tag{2}$$

and the corresponding result for C7 is presented in Fig. 5. In ordinary Sm-*A*, S_{app} can be considered as the molecular orientational order parameter $S\equiv\langle P_2\rangle$. In Sm-$C^*$, on the other hand, these are related by the equation [47,48]

$$S_{\text{app}} = SP_2(\cos\Theta), \tag{3}$$

where Θ is the director tilt angle and $P_2(\cos\Theta)$ is the second-order Legendre polynomial. Details will be discussed in Sec. III.

Repeating the above analysis, we obtain the $\langle P_2\rangle_{\text{app}} \equiv S_{\text{app}}$ values, for TSiKN65, shown in Fig. 6 (the solid black circles). Values of the tilt angle for this material have already been published [40]. Selecting a few such values for temperatures close to the Sm-*A* to sm-*C* transition, together with our measured values of $\langle P_2\rangle_{\text{app}}$, and using Eq. (3), we obtain the values of the true order parameter (the open black squares shown in Fig. 6). Taking these calculated values of $\langle P_2\rangle$ and assuming that the tilt is zero at the Sm-*A*-isotropic transition, we then interpolate values of $\langle P_2\rangle$ for the rest of the temperature range using the theory developed by Chirtoc *et al.* [41] (the red line in Fig. 6). The assumption of the tilt angle at the Sm-*A*-isotropic transition being zero can be justified in view of the fact that the hindered apparent rotational order parameter D_{app} is experimentally found to approach zero at this transition. The likely explanation of the latter result is that tilt angle at this transition must be zero. In any case, the tilt can be no less than zero, and consequently the interpolated values thus found can be regarded as being a lower bound for the tilt as a function of temperature. Finally, we use these interpolated values of $\langle P_2\rangle$ and Eq. (3) again to obtain the molecular tilt angles for the full range of temperatures (the dotted blue line in Fig. 6). It is clear that a large molecular tilt exists in the Sm-*A* phase of TSiKN65, at least

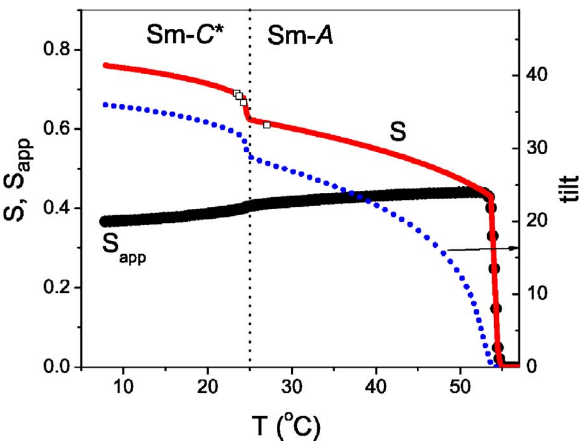

FIG. 6. (Color online) Apparent order parameter (black circles), true order parameter (red thicker line), and implied molecular tilt in degrees (dotted blue line) for TSiKN65, in a homeotropic cell.

30 °C near the transition to the Sm-*C* phase. This confirms TSiKN65 as a material that exhibits de Vries behavior, which allows us to conclude that some, though not all, systems with first-order Sm-*A*-Sm-*C** transitions are of the de Vries type.

We present a comparison of the apparent order parameter measurements, by IR absorbance, for TSiKN65 in homogeneous and homeotropic configurations, respectively. The homogeneous alignment is achieved using Nissan RN1266 polyimide coating, which is baked in an oven for 12 h at a temperature of 250 °C. The IR beam is incident along the X axis of the laboratory frame, and the absorbance A_Z is recorded along the layer normal in the Sm-*A* phase (the Z direction) and A_Y is recorded along the direction perpendicular to it (the Y direction). The set of equations (4), from the work of Merkel *et al.* [47], are used to analyze this data. In this calculation, we assume the order parameters $C=D=P=0$ and that the polar angle β between the C-C vibration of the benzene ring and the long molecular axis to be zero. Results are given in Fig. 7. Surprisingly, we find that the order parameter calculated from the absorbance A_Z varies from 0.25 to 0.3, whereas that calculated from A_Y is found to be almost constant (0.4) over the entire temperature range of the Sm-*A* phase, which is much closer to that found in the homeotropic configuration. These results show that the director of the sample may be tilted out of the plane of the window for TSiKN65. This may be one of the reasons for the rather low apparent order parameter already observed by Hayashi *et al.* [45] and by Collings *et al.* [42] using rather different techniques. The other may be large angle (~30 °) between the long molecular axis and the rigid core as discussed by Hayashi *et al.* [45].

For C7, S_{app} is fitted to the McMillan model [49] in Sm-*A* and reasonable fitting of the experimental results to the model shown in Fig. 8 is achieved. The ratio of the barrier height to the Boltzmann constant, V_0/k_B, and the positional order parameter τ are the fitting parameters, which are 1190 K and 0.34, respectively. These appear to be reasonable values for Sm-*A*. The standard deviation for the Gaussian distribution of the molecular fluctuation, σ, of the tilt angle as a function of temperature is also shown in Fig. 8.

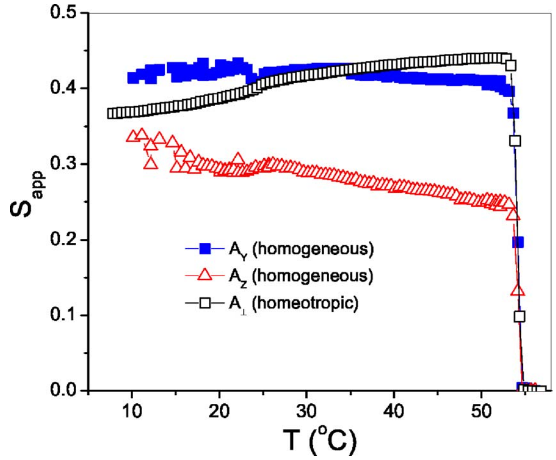

FIG. 7. (Color online) Comparison of the apparent order parameter measurements of TSiKN65 for homogeneous and homeotropic configurations, obtained by IR absorbance.

B. Polarized Raman spectroscopy in homogeneously aligned cells

A homogeneously aligned sandwich cell of 1.5 μm in thickness of the material C7 was prepared for polarized Raman scattering experiments. The material was introduced in the isotropic phase between two quartz glass substrates plated with indium tin oxide using the capillary effect. Those substrates were coated with ~20-nm-thick polyimide aligning films (Nissan, RN-1266), and only one of the substrates was rubbed in one direction and sense. The sample cell was mounted in an oven, the temperature of which was adjusted by a temperature controller (Yokogawa, UP550) within an accuracy of ±0.1 °C.

The micrograph captured in Sm-*C** is shown in Fig. 9. In the polarizing microscope observations, the smectic layer normal was found to tilt by an angle of about 5° from the rubbing direction due to the interface-induced electroclinic effect. The optical axis is tilted by an angle of about 18° with respect to the smectic layer normal $\hat{\boldsymbol{e}}$. The sufficiently dark

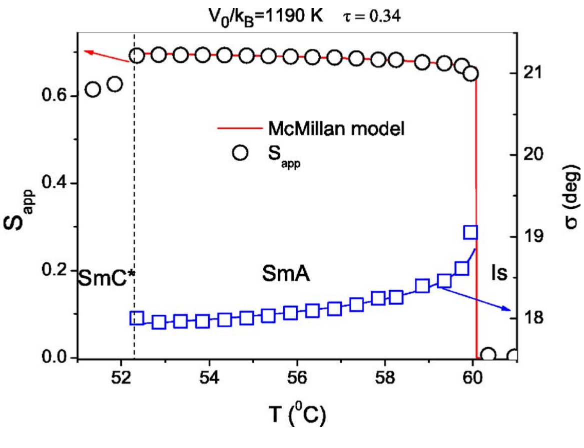

FIG. 8. (Color online) Orientational apparent S_{app} order parameter fitted to the McMillan model for the Sm-*A* phase of C7 and the standard deviation for the Gaussian distribution of the molecular fluctuations of the tilt as a function of temperature.

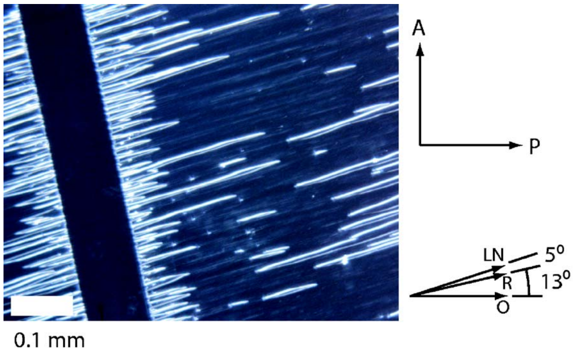

FIG. 9. (Color online) Micrograph image of the surface stabilized state at 46 °C in Sm-C^* for a 1.5-μm-thick sample cell containing C7. The white thick bar at the left bottom corner shows 0.1 mm length. The horizontal and vertical edges of the photograph are parallel to the polarizer and the analyzer of the microscope as shown by the arrows marked by P and A. The arrows indicated by R, LN, and O show the rubbing direction, layer normal, and optical axis, respectively. Vertical slanting dark thick bar is the spacer in between the two glass plates. The white lines are the borders of the so-called zigzag defects. Only one of the two domains emerges in the SSFLC cell without external field because only one of the cell surfaces is rubbed with the cell being asymmetrical.

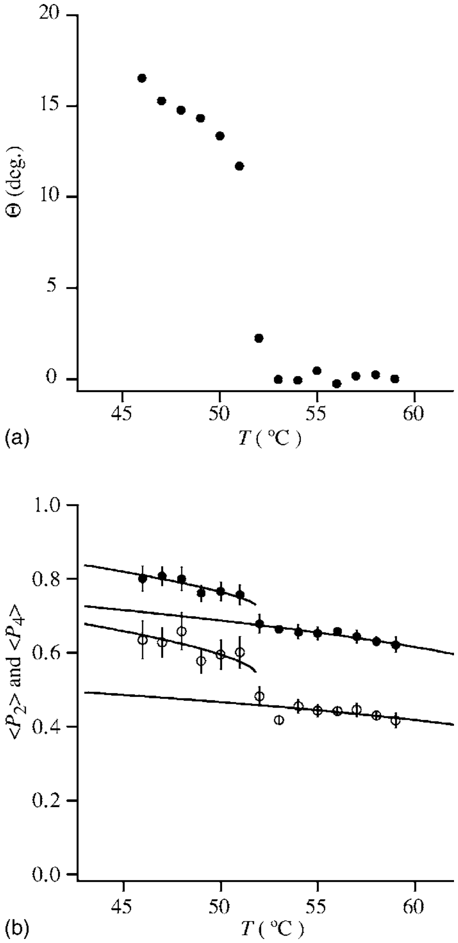

FIG. 10. (a) The apparent molecular tilt angle with respect to the layer normal determined from Raman experiments on C7, Θ_{app}, is plotted versus temperature T. The angle with reference to the layer normal is determined from the rotation angle where the Raman intensity polarized parallel to the incident laser polarization direction shows the maximum. (b) Orientational order parameters experimentally obtained by polarized Raman spectroscopy as a function of T in Sm-A and C^*. Solid and open circles denote $\langle P_2\rangle$ and $\langle P_4\rangle$, respectively. The lines are drawn as fits to Landau–de Gennes equations (9) and (13) as given in the section on discussion.

and uniform texture observed in places free from white lines, representing the zigzag defects, shows the realization of an ideal surface stabilized ferroelectric state with the absence of the helical structure. The polarized Raman measurements were carried out on such a well-aligned area confirmed beforehand by polarizing microscopy. The Raman line at 1605 cm^{-1}, assigned to the phenyl ring C-C stretching mode, was used for probing the molecular orientational ordering. The depolarization ratio of this Raman line in the isotropic phase (iso) was found to be 0.383. Details of the experimental setup and the method of obtaining the apparent orientational order parameters $\langle P_2\rangle_{\rm app}$ and $\langle P_4\rangle_{\rm app}$ are described in our previous papers [30,45].

The apparent in-layer director tilt angle $\Theta_{\rm app}$ was determined from the direction giving the maximum value of the parallel component of the polarized Raman intensity relative to the smectic layer normal $\hat{\boldsymbol{e}}$ [30]. The results are plotted in Fig. 10(a). The apparent director tilt angle stays at almost zero in Sm-A, jumps to ~12° at the Sm-A-Sm-C^* phase transition temperature, and gradually becomes larger at lower temperatures. The large discrepancy in the director tilt angle between Fig. 10(a) and Fig. 1 of Ref. [50] must be due to the presence of the ordinary vertical chevron structure [31] in the homogeneous aligned sample cell. The small difference in the director tilt angle determined from the Raman experiments and the optical observations of the texture [cf. Figs. 9 and 10(a)] may be due to a small twist and splay deformation of the in-layer director along the direction perpendicular to the substrate plates, which is caused by the chevron structure [31]. Figure 10(b) also shows the experimentally obtained apparent orientational order parameters. The in-layer director $\hat{\boldsymbol{n}}$ is tilted by Θ in a single direction in Sm-C^* and is parallel to the substrates if we neglect the aforementioned small twist and splay deformation. The effect of chevron structure is actually small as is shown in Sec. III. Typical errors in the analysis for $\langle P_2\rangle$ and $\langle P_4\rangle$ from cheveron structure are estimated to be equal to 0.03 and 0.05, respectively. Hence $\langle P_2\rangle_{\rm measured}$ and $\langle P_4\rangle_{\rm measured}$ thus obtained could be regarded as the real orientational order parameters $\langle P_2\rangle$ and $\langle P_4\rangle$. However, in the general case where the in-layer director could be tilted in Sm-A phase (which is under consideration here) and or there may be a cheveron structure in the cell, these parameters could be termed as the apparent $\langle P_2\rangle_{\rm app}$ and $\langle P_4\rangle_{\rm app}$ order parameters. Both $\langle P_2\rangle$ and $\langle P_4\rangle$ show temperature dependences similar to that already observed [31].

III. DISCUSSION

In Sm-C^* systems, both the real director tilt Θ and the fluctuational molecular tilt θ contribute to the apparent order

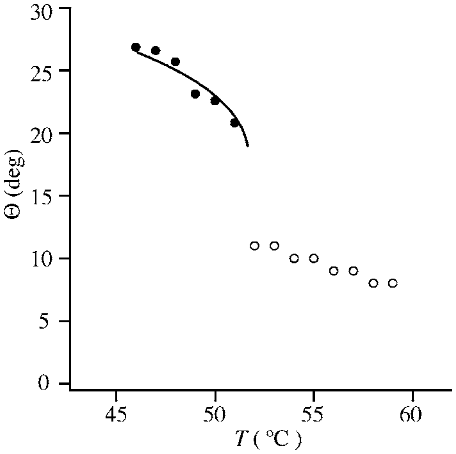

FIG. 11. Temperature dependence of Θ in C7. The values in open circles are calculated from Eq. (4) by taking the measured $\langle P_2\rangle$ and $\langle P_4\rangle$ values from Fig. 10(b). Values in solid circles are calculated using Eq. (3) as described in the text. The solid line is the prediction of the Landau model for the Sm-C^* phase [Eqs. (15) and (16)].

parameter $\langle P_2\rangle_{\mathrm{app}}$, obtained from IR spectroscopy in a homeotropic cell, as expressed by Eq. (3). If the orientational order parameter $\langle P_2\rangle$ obtained from polarized Raman spectroscopy of C7, as given in Fig. 10(b), is the true molecular orientational order parameter, we can obtain Θ as a function of temperature by using Eq. (3). The result shown in Fig. 11 (solid circles) is in good agreement with the one previously obtained by Bahr and Heppke, using a high electric field [50,51]. If we use the Θ thus obtained, then the apparent orientational order parameter $\langle P_2\rangle_{\mathrm{app}}$ determined by IR spectroscopy can be converted into the true $\langle P_2\rangle$. The result for the apparent orientational order parameter, given in Fig. 5, when corrected for the tilt angle, closely reproduces the corresponding $\langle P_2\rangle$ determined by polarized Raman spectroscopy. Thus, the temperature variations of real director tilt angle Θ and of the molecular orientational order parameter $\langle P_2\rangle$ are consistent with each other. Consequently, the conventional model for Sm-C^* can satisfactorily describe the properties of C7.

Now let us consider the two possible models for Sm-A. The in-layer directors $\hat{\boldsymbol{n}}$ are parallel to the smectic layer normal $\hat{\boldsymbol{e}}$ in ordinary Sm-A, whereas it is tilted from $\hat{\boldsymbol{e}}$ by an angle Θ and distributes randomly around $\hat{\boldsymbol{e}}$ to assure the uniaxiality in de Vries Sm-A. Let us first assume that the director tilt angle Θ does not change at the Sm-A-Sm-C^* phase transition. Since Sm-C^* has $\Theta=20°$ just below the phase transition from Sm-A, it is natural to consider that the true molecular order parameters $\langle P_2\rangle$ and $\langle P_4\rangle$ do not change. In the uniaxial de Vries Sm-A, the apparent order parameters are related to the true molecular order parameters by following equation:

$$\langle P_L\rangle_{\mathrm{app}} = P_L(\cos\Theta)\langle P_L\rangle, \quad L=2 \text{ and } 4. \tag{4}$$

This equation turns out to be rather similar and a generalization of Eq. (3). This is based on the concept that the in-layer director is distributed on the cone at an angle of Θ. By using Eq. (4) and assuming $\langle P_2\rangle=0.75$ and $\langle P_4\rangle=0.62$ as the molecular order parameters just below the Sm-A and Sm-C^* transition and for a cone angle of $\Theta=20°$, we calculate the apparent order parameters and obtain $\langle P_2\rangle_{\mathrm{app}}=0.62$ and $\langle P_4\rangle_{\mathrm{app}}=0.29$. These are found to be much smaller than those obtained using Raman spectroscopy in Sm-A. Clearly, the assumption is not correct. In order for the results to agree reasonably well, this would imply a much lower in-layer director tilt angle in Sm-A. The in-layer director tilt angle Θ in any case shows a discontinuous change at the phase transition. Let us consider conversely and try to calculate maximum possible Θ that can reproduce the observed $\langle P_2\rangle_{\mathrm{app}}$ and $\langle P_4\rangle_{\mathrm{app}}$ in the Sm-A temperature region given in Fig. 10. For the true molecular order parameters, we assume the largest possible values $\langle P_2\rangle$ and $\langle P_4\rangle$, which Sm-C^* has just below the Sm-A-Sm-C^* phase transition. The result is given in Fig. 11 (open circles). The in-layer director tilt angle Θ is found to be considerably small in the Sm-A temperature region. If we assume smaller values for $\langle P_2\rangle$ and $\langle P_4\rangle$, Θ becomes even much smaller in the temperature range of Sm-A.

Now let us return to the results of the IR measurements. The original data $A_\perp/A_{\mathrm{iso}}$ given in Fig. 2 clearly show a decrease (open circles) in the Sm-A temperature region. In other words, the corresponding $S_{\mathrm{app}}\equiv\langle P_2\rangle_{\mathrm{app}}$ clearly shows an increase in Fig. 5 with a reduction in temperature in Sm-A phase. The simplest and most straightforward interpretation is to consider ordinary Sm-A and to ascribe the decrease in $A_\perp/A_{\mathrm{iso}}$ or the increase in $S_{\mathrm{app}}\equiv\langle P_2\rangle_{\mathrm{app}}$ to the decrease of the fluctuational molecular tilt $\langle\theta\rangle$ with falling temperature. By assuming the Gaussian distribution for the tilt angle, we obtain the standard deviation of the tilt, σ, as a function of temperature. The fluctuational amplitude σ shows a monotonic decrease as temperature decreases. We clearly obtain a reasonable temperature dependence of σ over temperature range of Sm-A. We can also adopt McMillan model for Sm-A to reproduce the temperature dependence of the order parameter S_{app}. The solid line in Fig. 8 is the prediction of the McMillan model with the positional order parameter $\tau=0.34$ at temperatures just above Sm-C^* to Sm-A transition and decreasing to zero at the Sm-A to iso transition. Now the question that is left to answer is as to whether it is meaningful or even necessary to introduce any finite tilt of the in-layer directors in the Sm-A temperature region. The answer, based on the experimental results, is that the well-established ordinary Sm-A model, where the in-layer director $\hat{\boldsymbol{n}}$ is parallel to the smectic layer normal $\hat{\boldsymbol{e}}$, appears to be satisfactory in understanding of the order parameters obtained from IR and polarized Raman spectroscopy for C7.

The differences in the results of the tilt angle in Fig. 10(a) obtained using Raman spectroscopy and those in Fig. 11 (solid circles) using IR spectroscopy carried out on a homeotropically aligned cell in Sm-C^* may be due to the presence of vertical cheveron structure in a homogeneously aligned cell, and we would also like to evaluate the effect of such a vertical chevron structure on $\langle P_2\rangle_{\mathrm{app}}$ and $\langle P_4\rangle_{\mathrm{app}}$. The following relations are derived from Fig. 12:

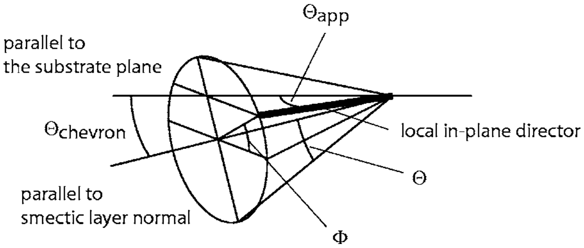

FIG. 12. Orientation of the local in-layer director at the alignment layer surface in chevron layer structure.

$$\frac{\sin \Theta \sin \Phi}{\cos \Theta} = \tan \Theta_{\text{chevron}} \tag{5}$$

and

$$\sin \Theta_{\text{app}} = \sin \Theta \cos \Phi . \tag{6}$$

Here Θ is the true in-layer director tilt angle obtained from IR measurements and Θ_{app} is the apparent tilt angle determined from the angle which gives the maximum intensity of the polarized Raman intensity I_z [Fig. 10(a)]. From Eqs. (5) and (6) the chevron angle is calculated as

$$\tan \Theta_{\text{chevron}} = \frac{\sqrt{\sin^2 \Theta - \sin^2 \Theta_{\text{app}}}}{\cos \Theta} . \tag{7}$$

Figure 13 shows the calculated chevron angles. By assuming that the twist and splay deformation of the in-layer directors is uniform, the effect of the chevron structure is estimated to be ∼+0.03 for $\langle P_2 \rangle$ and ∼+0.04 for $\langle P_4 \rangle$, which are within the error bars as shown in Fig. 10(b).

The necessity of de Vries Sm-*A* originates from two experimental facts observed across the Sm-*A*-Sm-*C* (Sm-C^*) phase transition. One is the small change in the smectic layer spacing in some compounds, and the other is the large increase in the birefringence at the transition temperature as well as a large increase in the birefringence with voltage in Sm-*A*. It should be noted that the smectic layer is the density wave and that almost all theoretical models could not *a priori* predict the wavelength—i.e., the layer spacing. In our opinion, it is too easy and too simplistic to ascribe the small change in the smectic layer spacing to a re-identification of the phase as de Vries Sm-*A*. This is particularly so in C7, the compound studied here. The smectic layer spacing shows a discontinuous change across the Sm-*A*-Sm-C^* transition (of 1.1 Å, which is approximately 3%), which that corresponds to a 15° jump in the in-layer director tilt angle [52]. It is also perhaps naive to consider that the spacing is determined by the well-defined molecular length and its tilting as those by rigid rods. There are so many factors which disturb this view. In particular, there are counterexamples where the layer spacing in a tilted phase becomes larger than that in the Sm-*A* phase [53].

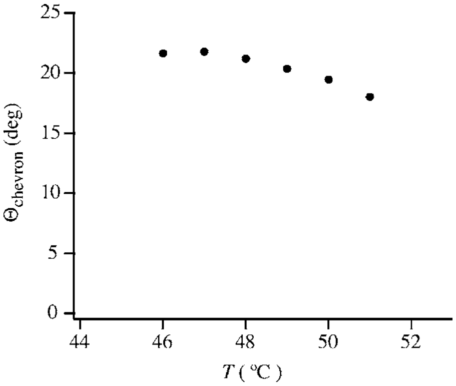

FIG. 13. Evaluated chevron layer tilt angle for the C7 cell.

Similarly, the large increase in the birefringence is not so unexpected. The true molecular order parameters usually become larger in Sm-C^* (Sm-*C*) than in Sm-*A* because of the coupling between Θ and $\langle P_2 \rangle$ and $\langle P_4 \rangle$. Let us consider this coupling rather in detail by using the Landau theory. The free energy of the orientational order, F_A, is assumed to be expandable in terms of the orientational order parameter $S \equiv \langle P_2 \rangle$ [9]:

$$F_A = f_{0,A} + \frac{1}{2}\alpha_A (T - T^*_{0,A}) S^2 + \frac{1}{3} b_A S^3 + \frac{1}{4} c_A S^4 . \tag{8}$$

Here $T^*_{0,A}$ is the hypothetical phase transition temperature between isotropic and Sm-*A*, $\alpha_A > 0$, $b_A < 0$, and $c_A > 0$ are the ordinary expansion coefficients describing the first-order transition, and *T* the absolute temperature. Note that the positional order parameter and its coupling with the orientational order parameter are not considered explicitly and included in the constant $f_{0,A}$. The equilibrium values of *S* are obtained by minimizing the free energy density:

$$S = \frac{-b_A + [b_A^2 - 4a_A c_A (T - T^*_{0,A})]^{1/2}}{2c_A} . \tag{9}$$

The iso-Sm-*A* phase transition temperature is obtained by substituting Eq. (9) into Eq. (8):

$$T_{\text{iA}} = \frac{2b_A^2 + 9a_A c_A T^*_{0,A}}{9a_A c_A} \tag{10}$$

under the conditions of $F_A - f_{0,A} = 0$ and $\partial F_A / \partial S = 0$. To extend the analysis, beyond the conventional $\langle P_2 \rangle$ theory, it is possible to expand the energy in powers of other moments of the orientational distribution function. For example, Lubensky and Radzihovsky [54] consider an expansion of the energy in powers of the first-, second-, and third-degree order parameters and their various cross coupling. Similarly, we extend our expansion of the energy to include powers of the fourth-degree ($U = \langle P_4 \rangle$) order parameter,

$$F_U = \frac{1}{2}\gamma_A (T - T^*_U) U^2 + \frac{1}{3} g_U U^3 + \frac{1}{4} h_U U^4 , \tag{11}$$

and the lowest-order cross coupling terms

$$F_{SU} = \frac{1}{2} m_A S^2 U + \frac{1}{2} n_A S U^2 . \tag{12}$$

Added together, these Eqs. (8), (11), and (12) form the lowest-order Landau energy of the second- and fourth-degree order parameters. This energy lacks any special symmetry: it is not symmetrical with respect to the exchange of *S* with −*S*,

TABLE I. Optimized Landau expansion coefficients and parameters.

Sm-A		Sm-C^*	
T_{iA} (°C)	60.0	T_{AC} (°C)	51.5
$T^*_{0,A}$ (°C)	−9.1	$T^*_{0,C}$ (°C)	50.8
$1/\lambda_A$	0.68 ± 0.01	$1/\lambda_C$	1.66 ± 0.06
		ζ	1.10 ± 0.04
a_A/c_A	0.011 ± 0.003	a_C/c_C	0.0024 ± 0.0008
b_A/c_A	-1.85 ± 0.03	b_C/c_C	-0.097 ± 0.012

the exchange of U with $-U$, the exchange of S with U. Consequently, the relationship of the equilibrium value of S to the equilibrium value of U will also be devoid of any particular symmetry. Hence, if we make a Taylor expansion of the equilibrium value of U in powers of S, we must expect that the lowest-order term will be linear. Fitting our experimental data to such a (lowest-order) linear relationship, we find

$$\langle P_4\rangle \simeq (0.68\pm0.01)\langle P_2\rangle. \tag{13}$$

The orientational order parameters obtained experimentally are reproduced by using Eqs. (9) and (13). The best-fit results are shown in Fig. 10(b) as solid lines, and the optimized Landau expansion coefficients are summarized in Table I, together with the ratio $\langle P_4\rangle/\langle P_2\rangle = 1/\lambda_A$. The very large temperature difference for the Iso-Sm-A phase transition, $T^*_{iA} - T_{O,A} = 69.1$ °C, may possibly result from the fact that, unlike the analysis performed for Fig. 8, the positional order parameter and its coupling with S have been neglected.

In describing the Sm-A-Sm-C^* phase transition, the Landau free energy density is usually written in terms of the in-layer director tilt angle Θ, after renormalizing the coupling between Θ and spontaneous polarization P_S [55],

$$F_C = \frac{1}{2}\alpha_C(T - T^*_{0,C})\Theta^2 + \frac{1}{4}b_C\Theta^4 + \frac{1}{6}c_C\Theta^6. \tag{14}$$

Here $T^*_{0,C}$ is the hypothetical phase transition temperature between Sm-A and Sm-C^*, $\alpha_C > 0$, $b_C < 0$, and $c_C > 0$ are the ordinary expansion coefficients describing the first-order transition, and T the absolute temperature. Minimizing Eq. (14), the equilibrium value of Θ is obtained as

$$\Theta^2 = \frac{-b_C + [b_C^2 - 4a_Cc_C(T - T^*_{0,C})]^{1/2}}{2c_C}. \tag{15}$$

The Sm-A-Sm-C^* phase transition temperature T_{AC} is given by substituting Eq. (15) into Eq. (14):

$$T_{AC} = \frac{3b_C{}^2 + 16a_Cc_CT^*_{0,C}}{16a_Cc_C}. \tag{16}$$

The in-layer tilt angle Θ obtained experimentally is well reproduced by using Eqs. (15) and (16). The best-fit results are shown in Fig. 11 as a solid line, and the optimized Landau expansion coefficients are summarized in Table I.

It is clear from Fig. 14(a) that the orientational order parameters in the C phase, $\langle P_2\rangle_C$ and $\langle P_4\rangle_C$, do not lie on the best-fitted curves of the A-phase order parameters, $\langle P_2\rangle_A$ and $\langle P_4\rangle_A$. This proves that there exists a coupling between the orientational order parameters and the in-layer director tilt Θ. Using the orientational order parameters measured immediately above and below the Sm-A-Sm-C transition, let us define

$$\delta_{P2} = \langle P_2\rangle_C - \langle P_2\rangle_A, \tag{17}$$

$$\delta_{P4} = \langle P_4\rangle_C - \langle P_4\rangle_A. \tag{18}$$

On the basis of the same arguments as for Eq. (13), we expect (as a first approximation) a linear relationship between the quantities defined in Eqs. (17) and (18). Fitting the data, we thus obtain

$$\delta_{P4} = (1/\lambda_C)\delta_{P2} \simeq (1.66\pm0.06)\delta_{P2}. \tag{19}$$

The problem of analyzing the coupling between the tilt Θ and an orientational order parameter, like $\langle P_2\rangle$, is much more complicated. A full analysis would require a coupling of the orientational and positional order parameters, from which the tilt should emerge to describe the relative orientation of the symmetry axes of the two types of order. However, the existing Landau theoretical order parameters are inappropriate: orientational order is described by a second-degree tensor,

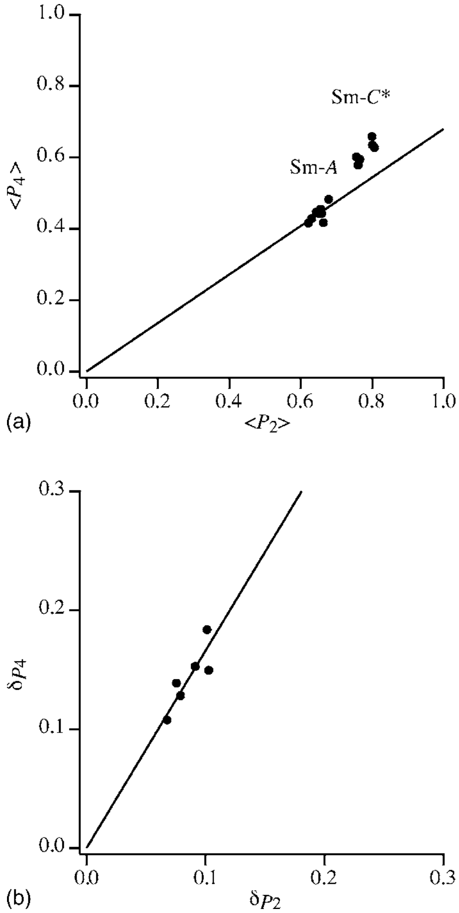

FIG. 14. (a) $\langle P_4\rangle$ is plotted against $\langle P_2\rangle$ and (b) δ_{P2} is plotted against δ_{P4} for the material C7. The definitions of δ_{P2} and δ_{P4} are given in the text.

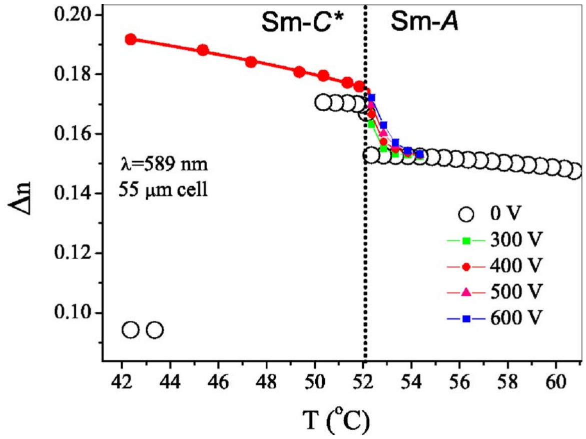

FIG. 15. (Color online) Birefringence of C7 measured at various electric field strengths in the smectic *A* and *C* phases.

while the positional order parameter is a complex scalar [9] and clearly one cannot obtain an orientationally nontrivial coupling of any tensor with a scalar. Instead, we proceed according to a symmetry argument. The ground state of the Sm-*A* phase, about which we wish to make a Landau expansion, has D_∞ symmetry. This is the same symmetry as $\langle P_2 \rangle$, so all powers of $\langle P_2 \rangle$, both odd and even, may be included in the expansion. Conversely, as the tilt breaks the D_∞ symmetry, not all powers of Θ will be acceptable in the energy. States with a tilt of either Θ or $-\Theta$ are physically indistinguishable, as one may be transformed into the other by rotating the system about the layer normal axis by 180°. Consequently, as $\Theta \rightarrow -\Theta$ is a symmetry operation for the energy, all odd powers of Θ must be absent from the energy and the lowest-order invariant in the expansion of δ_{P2} in powers of Θ will be quadratic:

$$\delta_{P2} = \zeta \Theta^2. \tag{20}$$

Fitting our data to these equations we find $\zeta = 1.10 \pm 0.04$. Given this, we find that Eqs. (17)–(19) reproduce $\langle P_2 \rangle_C$ and $\langle P_4 \rangle_C$ well, as illustrated in Fig. 14(b). The important point is that this proves that there exists a coupling between the in-layer director tilt angle Θ and the true molecular order parameters $\langle P_2 \rangle$ and $\langle P_4 \rangle$. Furthermore, we anticipate that this coupling should be responsible for a large change in birefringence. We measure the birefringence change by using the electroclinic effect—i.e., the electric-field-induced Sm-C^* (Fig. 15). It should be noted that the large Goldstone-mode fluctuations of the azimuthal angle Φ of the in-layer director, which would otherwise be present, are completely suppressed by the applied field and this suppression also results in a large increase in birefringence with voltage. The large value of birefringence in the Sm-C^* phase of C7 at zero applied field is unusual: normally one would expect the helical structure to reduce the birefringence to almost zero. In this case, we have unwound metastable domains in the Sm-C^*, which persist for some time after the Sm-*A*-Sm-C^* transition has taken place. We note that two much smaller values of birefringence are measured (for zero applied field) a short time later and at a lower temperature of between 42 and 44 °C, once the system has had some time to relax towards it equilibrium structure.

IV. SUMMARY

Topical discussions taking place at international conferences, symposia, and in the literature have suggested that the Sm-*A* phase in compounds that show first order Sm-*A* to Sm-C^* transitions are possibly of the de Vries type. In this type, the in-layer director is tilted from the smectic layer normal $\hat{\boldsymbol{e}}$ by an angle of Θ but is distributed randomly around $\hat{\boldsymbol{e}}$ on a cone to assure the uniaxiality of Sm-*A*. To establish whether smectics with a first-order Sm-*A*-Sm-C^* must belong to the de Vries type we have investigated two such materials: C7 and the organosiloxane TSiKN65. For C7, our IR and Raman scattering results can be explained in terms of a conventional Sm-*A* phase. The sudden increase in the birefringence at the Sm-*A* to Sm-C^* transition may arise because of the jump in the orientational order parameter $\langle P_2 \rangle$ which occurs because it is coupled to the tilt, which itself undergoes a jump discontinuity at the transition to the Sm-C^* phase. The IR results in particular show that the in-layer director in Sm-*A*, even at a microscopic level, is not tilted with respect to the layer normal and that the tilt suddenly appears at the transition from Sm-*A* to Sm-C^*. This is further confirmed by the temperature dependence of the IR absorbance across the temperature range of Sm-*A* phase. The Raman scattering results allow us to calculate the orientational order parameters $\langle P_2 \rangle$ and $\langle P_4 \rangle$, and we have investigated the couplings between them and between $\langle P_2 \rangle$ and the tilt angle Θ. This latter coupling appears to be responsible for the increase in the birefringence at the transition to Sm-C^*. Conversely, de Vries phases have been shown to exist in some compounds [35–37,40,45,56] and we can confirm TSiKN65 belongs to this list, as our IR absorbance results show very clear de Vries behavior for this material. We conclude that IR and Raman spectroscopy can play a central role in determining the existence of a de Vries Sm-*A* phase, but that behavior such as a first-order Sm-*A* to Sm-C^* transition or a large change in the birefringence at this transition, while necessary characteristics, are not sufficient evidence to constitute proof that a particular material has a de Vries phase.

ACKNOWLEDGMENTS

We would like to thank I. Kobayashi of Nissan Chemical Industries, Ltd. for supplying the aligning agent (Nissan, RN-1266). J.K.V. thanks the Science Foundation of Ireland for Grant No. SFI (02/In.1/I031) for funding the research and visit of N.H. to Dublin and the visiting appointment of A. Kocot. M.J.L. thanks the European Union for funding under the SAMPA programme (HPRN-CT-2002-00202). Atsuo Fukuda's research at Trinity College Dublin was funded by Grant No. SFI (02/W/I02).

[1] B. W. van der Meer and G. Vertogen, J. Phys. (Paris) **40**, C3–222 (1979).
[2] A. S. Govind and N. V. Madhusudana, Europhys. Lett. **55**, 505 (2001).
[3] A. S. Govind and N. V. Madhusudana, Eur. Phys. J. E **9**, 107 (2002).
[4] R. G. Priest, J. Chem. Phys. **65**, 408 (1976).
[5] M. A. Osipov and S. A. Pikin, Mol. Cryst. Liq. Cryst. **103**, 57 (1983).
[6] W. J. A. Goossens, Mol. Cryst. Liq. Cryst. **150**, 419 (1987).
[7] A. Poniwierski and T. J. Sluckin, Mol. Phys. **73**, 199 (1991).
[8] M. A. Osipov, A. Fukuda, and H. Hakoi, Mol. Cryst. Liq. Cryst. **402**, 6 (2003).
[9] P. G. de Gennes and J. Prost, *The Physics of Liquid Crystals* (Clarendon Press, Oxford, 1993).
[10] W. L. McMillan, Phys. Rev. A **8**, 1921 (1973).
[11] R. J. Meyer and W. L. McMillan, Phys. Rev. A **9**, 899 (1974).
[12] A. Wulf, Phys. Rev. A **11**, 365 (1975).
[13] W. J. A. Goossens, J. Phys. (Paris) **46**, 1411 (1985).
[14] M. Matsushita, J. Phys. Soc. Jpn. **47**, 331 (1977).
[15] W. H. de Jeu and J. A. de Poorter, Phys. Lett. **61A**, 114 (1977).
[16] A. de Vries, Mol. Cryst. Liq. Cryst. **41**, 27 (1977).
[17] A. Wulf, Phys. Rev. A **17**, 2077 (1978).
[18] A. de Vries, J. Chem. Phys. **71**, 25 (1979).
[19] A. de Vries, A. Ekachai, and N. Spielberg, Mol. Cryst. Liq. Cryst. Lett. **49**, 143 (1979).
[20] A. de Vries, A. Ekachai, and N. Spielberg, J. Phys. (Paris), Colloq. **40**, C3-147 (1979).
[21] A. D. L. Chandani, Y. Ouchi, H. Takezoe, A. Fukuda, K. Terashima, K. Furukawa, and A. Kishi, Jpn. J. Appl. Phys., Part 2 **28**, L1261 (1989).
[22] A. Fukuda and H. Takezoe, *Structures and Properties of Ferroelectric Liquid Crystals* (Corona, Tokyo, 1990), pp. 174–193, and references therein.
[23] Y. Takanishi, A. Ikeda, H. Takezoe, and A. Fukuda, Phys. Rev. E **51**, 400 (1995).
[24] M. A. Osipov and A. Fukuda, Phys. Rev. E **62**, 3724 (2000).
[25] A. Fukuda, H. Hakoi, M. Sato, and M. A. Osipov, Mol. Cryst. Liq. Cryst. **398**, 169 (2003).
[26] E. Gorecka, D. Pociecha, M. Glogarova, and J. Mieczkowski, Phys. Rev. Lett. **81**, 2946 (1998).
[27] D. Pociecha, M. Glogarova, E. Gorecka, and J. Mieczkowski, Phys. Rev. E **61**, 6674 (2000).
[28] A. Fukuda, H. Hakoi, T. Okugawa, T. Matsumoto, Y. Suzuki, M. Johno, N. Hayashi, T. Kato, S. Kawada, and S. Kondoh, S. Kondoh, in *Proceedings of the Asia Display/IDW 01, Nagoya, Japan* (Society for Information Display, San Jose, CA, 2001), p. 77.
[29] N. Hayashi, T. Kato, T. Aoki, T. Ando, A. Fukuda, and S. S. Seomun, Phys. Rev. Lett. **87**, 015701 (2001).
[30] N. Hayashi, T. Kato, T. Aoki, T. Ando, A. Fukuda, and S. S. Seomun, Phys. Rev. E **65**, 041714 (2002).
[31] N. Hayashi, T. Kato, T. Ando, A. Fukuda, S. Kawada, and S. Kondoh, Phys. Rev. E **68**, 011702 (2003).
[32] N. Hayashi, T. Kato, T. Aoki, T. Ando, A. Fukuda, and S. S. Seomun, Phys. Rev. Lett. **91**, 239602 (2003).
[33] A. Fukuda, Proceedings of Asia Display 95, Hamamatsu, Japan (Society for Information Display, San Jose, CA, 1995), p. 61.
[34] S. Inui, N. Iimura, T. Suzuki, H. Iwane, K. Miyachi, Y. Takanishi, and A. Fukuda, J. Mater. Chem. **6**, 671 (1996).
[35] Yu. P. Panarin, V. Panov, O. E. Kalinovskaya, and J. K. Vij, J. Mater. Chem. **9**, 2967 (1999).
[36] N. A. Clark, T. Bellini, R.-F. Shao, D. Coleman, S. Bardon, D. R. Link, J. E. Maclennan, X.-H. Chen, M. D. Wand, D. M. Walba, P. Rudquist, and S. T. Lagerwall, Appl. Phys. Lett. **80**, 4097 (2002).
[37] O. E. Panarina, Yu. P. Panarin, J. K. Vij, M. S. Spector, and R. Shashidhar, Phys. Rev. E **67**, 051709 (2003).
[38] C. S. O'Hern, T. C. Lubensky, and J. Toner, Phys. Rev. Lett. **83**, 2745 (1999).
[39] M. S. Spector, P. A. Heiney, J. Naciri, B. T. Weslowski, D. B. Holt, and R. Shashidhar, Phys. Rev. E **61**, 1579 (2000).
[40] J. V. Selinger, P. J. Collings, and R. Shashidhar, Phys. Rev. E **64**, 061705 (2001).
[41] I. Chirtoc, M. Chirtoc, C. Glorieux, and J. Thoen, Liq. Cryst. **31**, 229 (2004).
[42] P. J. Collings, B. R. Ratna, and R. Shashidhar, Phys. Rev. E **67**, 021705 (2003).
[43] F. Giesselmann (private communication) and (unpublished).
[44] R. B. Meyer and R. A. Pelcovits, Phys. Rev. E **65**, 061704 (2002).
[45] N. Hayashi, T. Kato, A. Fukuda, J. K. Vij, Yu. P. Panarin, J. Naciri, R. Shashidhar, S. Kawada, and S. Kondoh, Phys. Rev. E **71**, 041705 (2005).
[46] J. Naciri, J. Ruth, G. Crawford, R. Shashidhar, and B. R. Ratna, Chem. Mater. **7**, 1397 (1994).
[47] K. Merkel, A. Kocot, J. K. Vij, G. H. Mehl, and T. Meyer, J. Chem. Phys. **121**, 5012 (2004).
[48] R. Korlacki, A. Fukuda, J. K. Vij, A. Kocot, V. Görtz, M. Hird, and J. W. Goodby, Phys. Rev. E **72**, 041704 (2005).
[49] S. Chandrasekhar, *Liquid Crystals* (Cambridge University Press, Cambridge, England, 1992).
[50] Ch. Bahr and G. Heppke, Phys. Rev. A **39**, 5459 (1989).
[51] Ch. Bahr and G. Heppke, Phys. Rev. A **41**, 4335 (1990).
[52] B. R. Ratna, R. Shashidhar, G. G. Nair, S. K. Prasad, C. Bahr, and G. Heppke, Phys. Rev. A **37**, 1824 (1988).
[53] Y. Takanishi, H. Takezoe, and A. Fukuda, Ferroelectrics **147**, 135 (1993).
[54] T. C. Lubensky and L. Radzihovsky, Phys. Rev. E **66**, 031704 (2002).
[55] A. Kocot, R. Wrzalik, J. K. Vij, M. Brehmer, and R. Zentel, Phys. Rev. B **50**, 16346 (1994).
[56] O. E. Panarina, Yu. P. Panarin, F. Antonelli, J. K. Vij, M. Reihmann, and G. Galli, J. Mater. Chem. **16**, 842 (2006).